Electronic Supplementary Material (ESI) for Energy & Environmental Science.
This journal is © The Royal Society of Chemistry 2016

Supplementary Material (ESI) for Energy & Environmental Science
This journal is © The Royal Society of Chemistry

A 3D bi-functional porous N-doped carbon microtube sponge electrocatalyst for oxygen reduction and oxygen evolution reactions

Jin-Cheng Li,† Peng-Xiang Hou,† Shi-Yong Zhao, Chang Liu,* Min Cheng, Feng Zhang, Hui-Ming Cheng

Shenyang National Laboratory for Materials Science, Institute of Metal Research, Chinese Academy of Sciences, Shenyang 110016, P. R. China.

E-mail: cliu@imr.ac.cn; Fax: +86-24-23903126; Tel: +86-24-83978280

ELECTRONIC SUPPLEMENTARY INFORMATION

Experimental section

1.1 Synthesis of the NCMT sponges

Facial cotton (100% cotton, Suzuran, Nagoya, Japan) was immersed in a mixture of ethanol and deionized water for 2 h at 80 °C to remove surface impurities. It was then washed and dried at 80 °C for one day before being placed in a quartz boat at the center of a 35-mm-diameter quartz tube in a horizontal tube furnace. The furnace temperature was raised to the desired pyrolysis temperatures at a rate of 15 °C/min under a 200 standard cubic centimeter per minute (sccm) NH_3 flow and the temperature remained constant for 1 h. NCMT-800, NCMT-900, NCMT-1000, and NCMT-1100 materials were obtained using pyrolysis temperatures of 800, 900, 1000, and 1100 °C, respectively. Finally, the furnace was cooled naturally to room temperature under the NH_3 atmosphere.

1.2 Material characterization

The morphology and structure of the NCMTs were characterized using scanning electron microscopy (SEM, Nova NanoSEM 430, operated at 15 kV), X-ray diffraction (XRD, Rigaku diffractometer with CuKα radiation), X-ray photoelectron

spectroscopy (XPS, Escalab 250, Al Kα), thermogravimetric analysis (NETZSCH STA 449C), Raman spectroscopy (Jobin Yvon HR800), and transmission electron microscopy (TEM, Tecnai F20 and Hitachi S4800, 200 kV). Electron energy loss spectroscopy (ELSS) was based on an energy-filtering TEM with the so-called "omega filter". The specific surface area and pore structure of the samples were investigated with an automatic volumetric sorption analyzer (ASAP 2020 M) using N_2 as the adsorbate at -196 ^oC.

1.3 Electrode preparation and electrochemical measurements

All the electrochemical measurements were performed on an electrochemical analysis station (CHI 760 E, CH Instruments, China) at room temperature using a standard three-electrode cell. A Pt wire and an Ag/AgCl electrode in saturated KCl served as the counter and reference electrodes, respectively. All the potentials in this study refer to that of a reversible hydrogen electrode (RHE). The potential difference between Ag/AgCl and RHE were based on a calibration measurement in H_2 saturated 0.1 M KOH with Pt wire as the working and counter electrodes, and Ag/AgCl as the reference electrode. A rotating disk electrode (RDE) with a glassy disk (5.0 mm diameter) and a rotating ring-disk electrode (RRDE) with a glassy carbon disk (5.61 mm diameter) and a Pt ring (6.25 mm inner-diameter and 7.92 mm outer-diameter) served as the substrate for the working electrode for evaluating the ORR and OER performance.

To prepare the working electrode, 4.0 mg of the catalysts (including reference catalysts: Pt/C (20 wt% of Pt, Alfa Aesar) and Ir/C (20 wt% of Ir, Premetek Co.) were ultrasonically dispersed in an ethanol solution containing 0.05 wt% Nafion (1.0 ml) to form a concentration of 4.0 mg/ml catalyst ink. A certain volume of catalyst ink was then pipetted onto the surface of a glassy carbon disk. The volumes of catalyst ink were 5 and 10 μL for the cyclic voltammetric (CV) and RDE/RRDE tests, respectively. The CV and RDE/RRDE tests were carried out in an O_2-saturated 0.1 M KOH solution. The scan rate was 100 mV s^{-1} for CV measurements and was 5 mV s^{-1} for the RDE/RRDE tests.

For the RDE tests, the polarization curves were collected at disk rotation rates of 400, 800, 1200, 1600, 2000, and 2500 rpm. For the calculation of the number of electrons transferred (n), we analyzed the kinetic parameters on the basis of the Koutecky–Levich equations:

$$\frac{1}{J} = \frac{1}{J_L} + \frac{1}{J_K} = \frac{1}{B\omega^{1/2}} + \frac{1}{J_K}$$

$$B = 0.62nFC_0(D_0)^{2/3}\nu^{-1/6}$$

$$J_K = \frac{1}{nkFC_0}$$

where J is the measured current density, J_K and J_L are the kinetic- and diffusion-limiting current densities, ω is the angular velocity, F is the Faraday constant ($F = 96500$ C/mol), C_0 is the bulk concentration of O_2 ($C_0 = 1.2\times10^{-6}$ mol/cm^3), D_0 is the diffusion coefficient of O_2 in 0.1 M KOH solution ($D_0 = 1.9\times10^{-5}$ cm^2/s), ν is the kinematic viscosity of the electrolyte (ν =0.01 cm^2/s), and k is the electron-transfer rate constant. For the Tafel plot, the kinetic current was calculated from the mass-transport correction of RDE by:

$$J_K = \frac{J_L \times J}{(J_L - J)}$$

For the RRDE tests, the polarization curves were collected at a disk rotation rate of 1600 rpm. The potential of the ring was set at 1.36 V (vs. RHE). The collecting efficiency of the RRDE (N) was 0.37. The peroxide yield (HO_2^-%) and the electron transfer number (n) was calculated as follows:

$$HO_2^- \% = 200 \times \frac{I_r / N}{I_d + I_r / N}$$

$$n = 4 \times \frac{I_d}{I_d + I_r / N}$$

where I_d is the disk current and I_r is the ring current.

The materials' resistance to the methanol crossover effect and its stability were tested in the same setup as for the RDE test in the O_2-saturated 0.1 M KOH aqueous electrolyte. The stability test was performed at a static potential of 0.5 V (vs. RHE) for the chronoamperometry at room temperature with the working electrode rotating at 1600 rpm.

For testing the catalyst with a 3D structure (denoted NCMT-1000 (3D)), NCMT-1000 sponge (~0.2 mg) was carefully cut to match the area of a glassy carbon electrode and then attached to the glassy carbon electrode using Nafion. The 2D structure of NCMT-1000 was prepared by commonly dropping 10 μL NCMT-1000 ink (4.0 mg/ml) and then drying. This process was repeated 5 times to obtain the same loading mass of the NCMT-1000 (3D) and NCMT-1000 electrodes. The RRDE for ORR tests was performed in an O_2-saturated 0.1 M KOH solution at a disk rotation rate of 1600 rpm. The scan rate was 5 mV s^{-1}.

The polarization curves of RDE voltammograms for the OER tests were collected in an O_2-saturated 0.1 M KOH solution at a disk rotation rate of 1600 rpm. The scan rate was 5 mV s^{-1}.

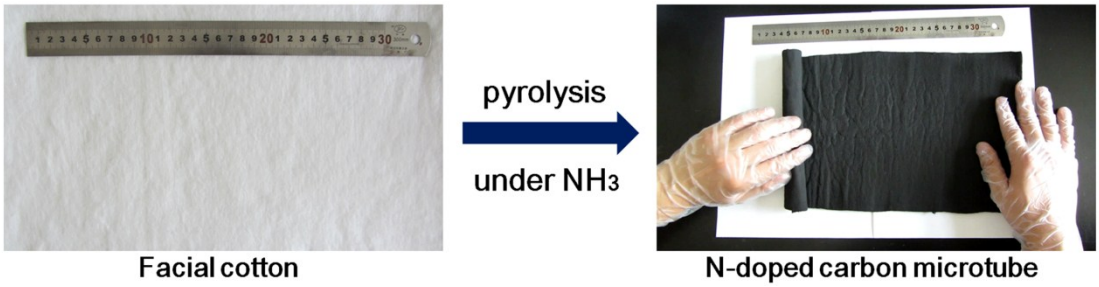

Fig. S1. Optical images of the facial cotton before and after the pyrolysis under an NH_3 atmosphere.

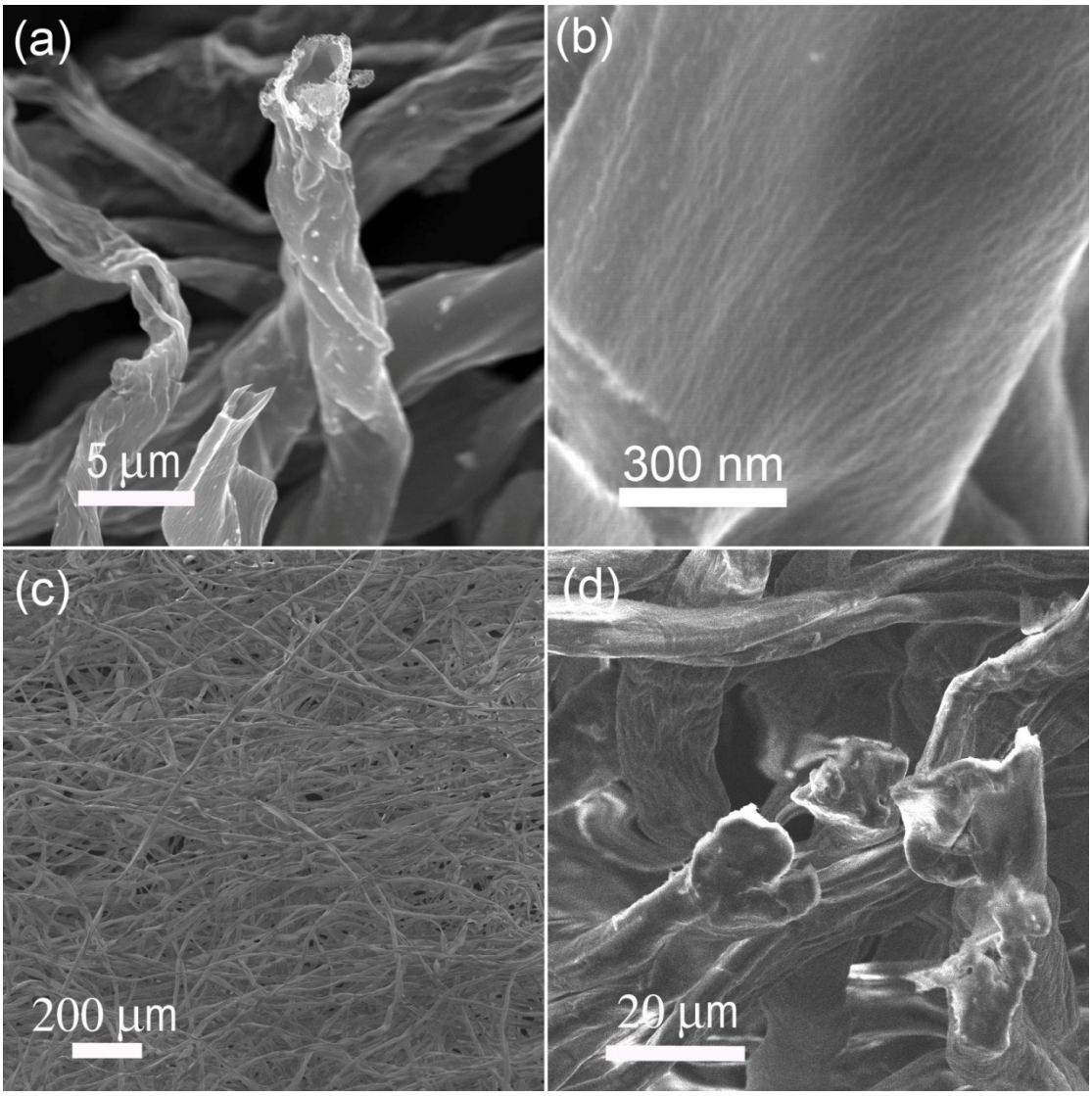

Fig. S2. SEM images of (a, b) NCMT-1000 and (c, d) facial cotton.

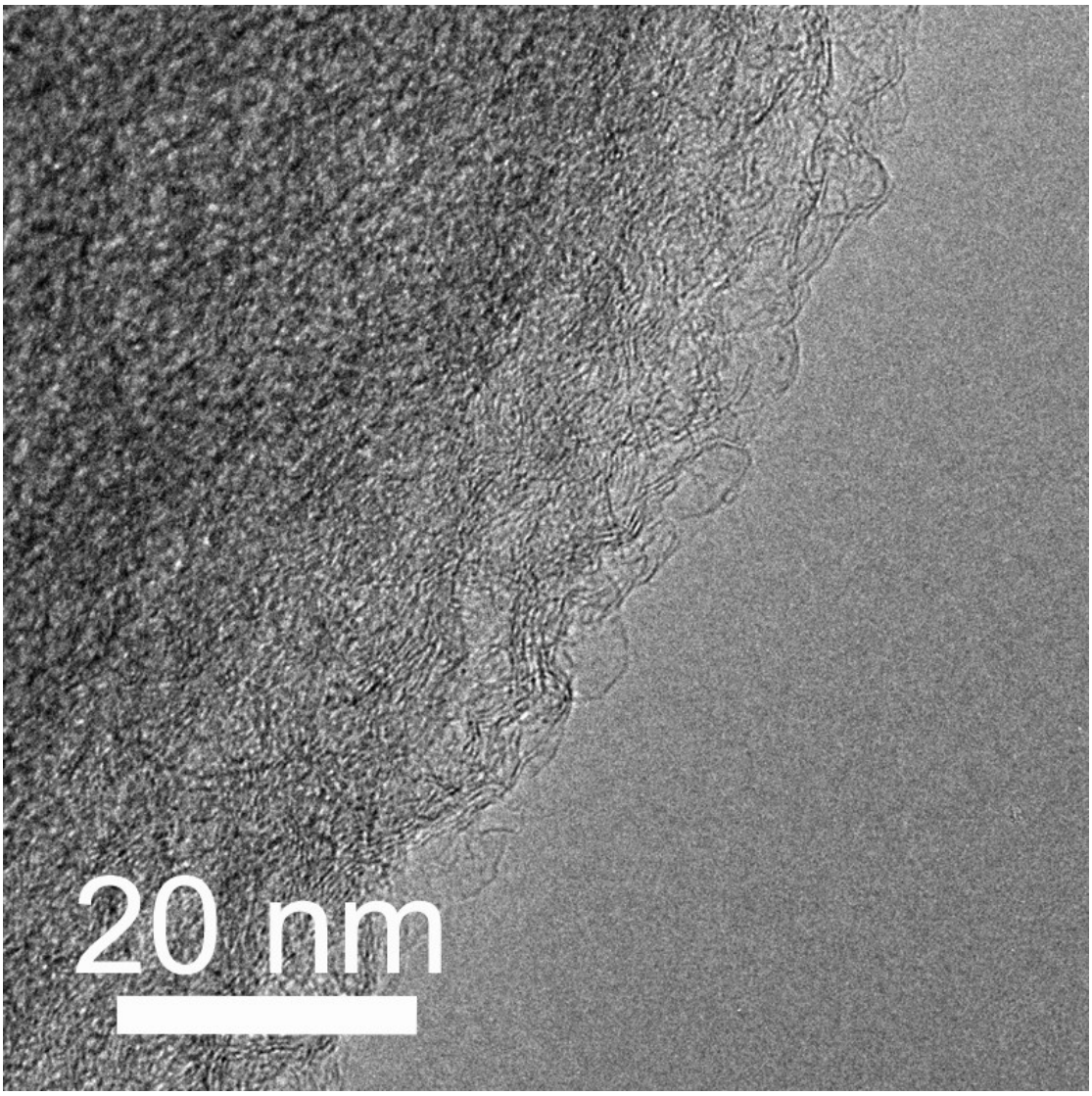

Fig. S3. TEM image of NCMT-1000.

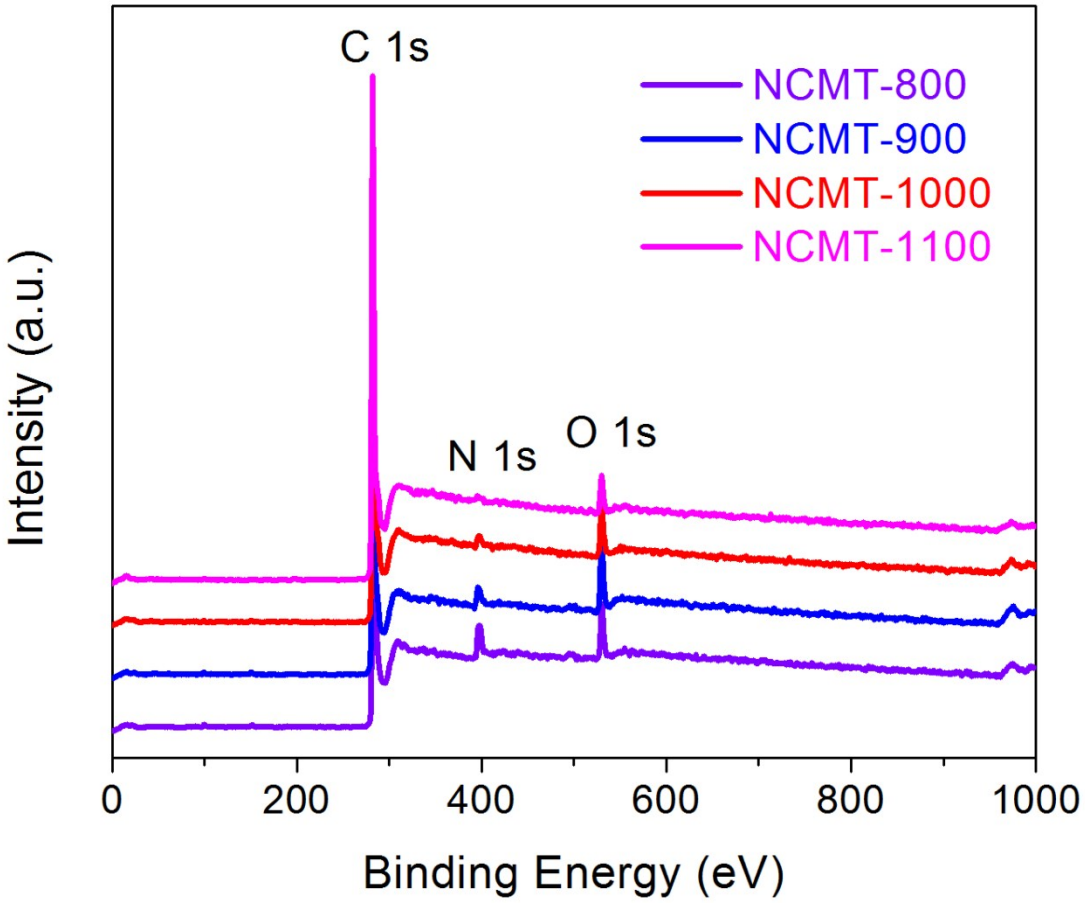

Fig. S4. XPS spectra of N1s of NCMT-800, NCMT-900, NCMT-1000, and NCMT-1100.

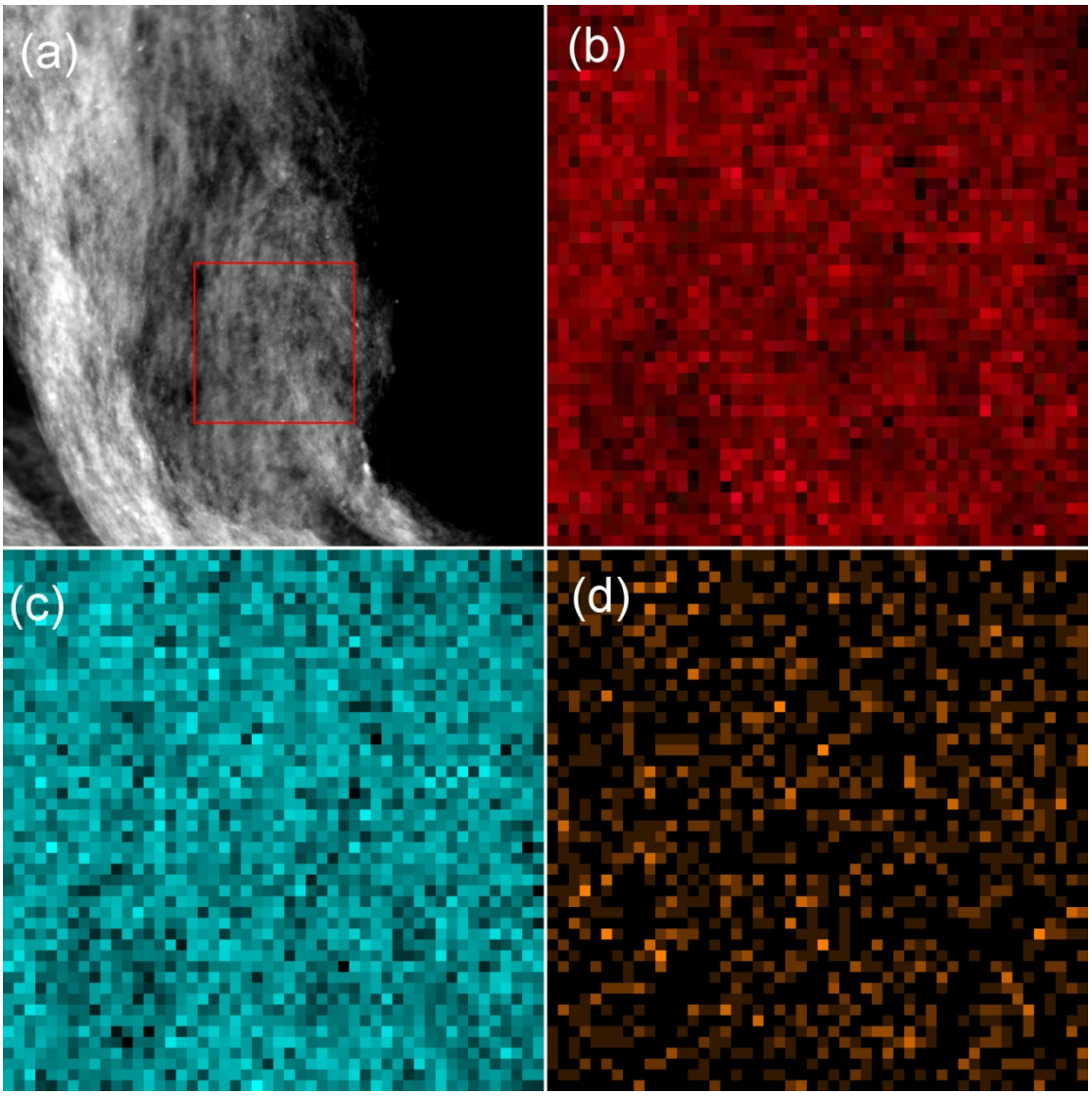

Fig. S5. (a) STEM image of NCMT-1000 and the corresponding elemental maps of (b) C, (c) N, and (d) O within the square area in (a).

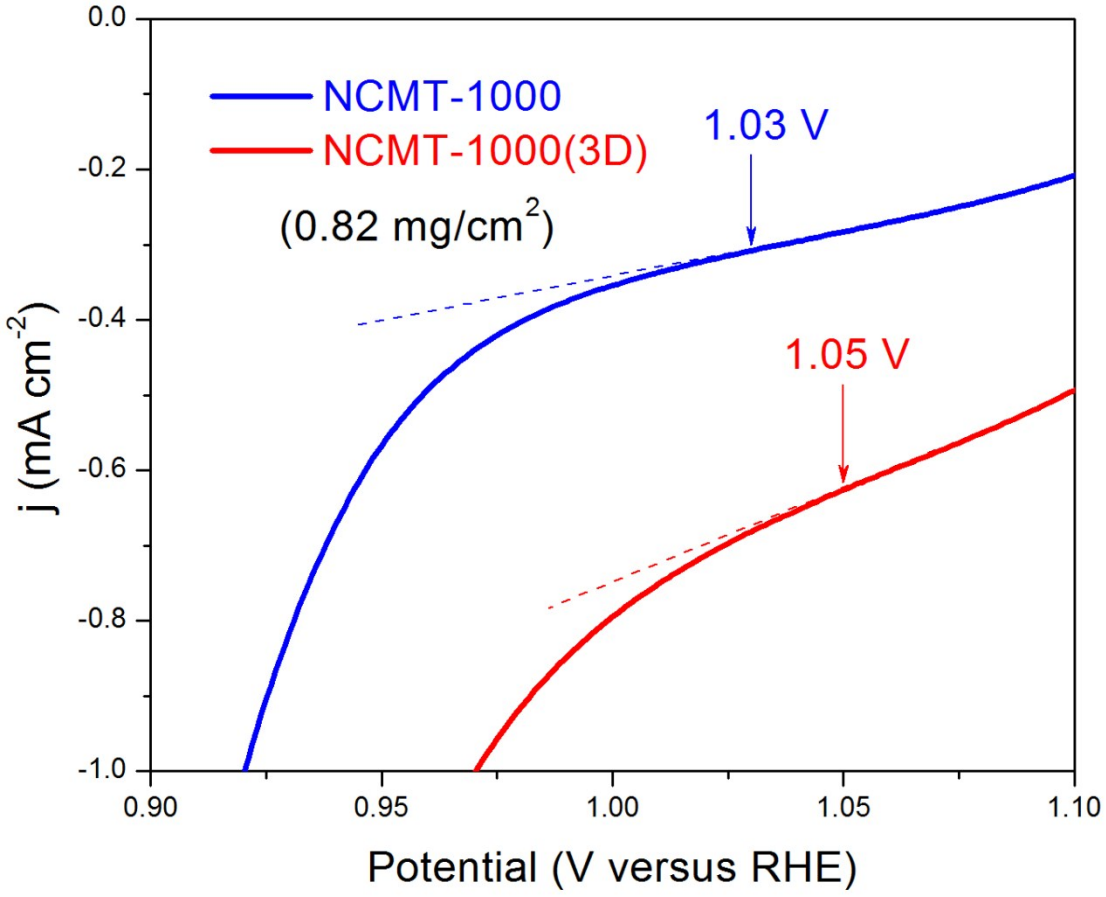

Fig. S6. RRDE polarization curves for the ORR of NCMT-1000 and NCMT-1000 (3D) in an O_2-saturated 0.1 M KOH solution at 1600 rpm. The catalyst loading was ~0.82 mg cm^{-2}.

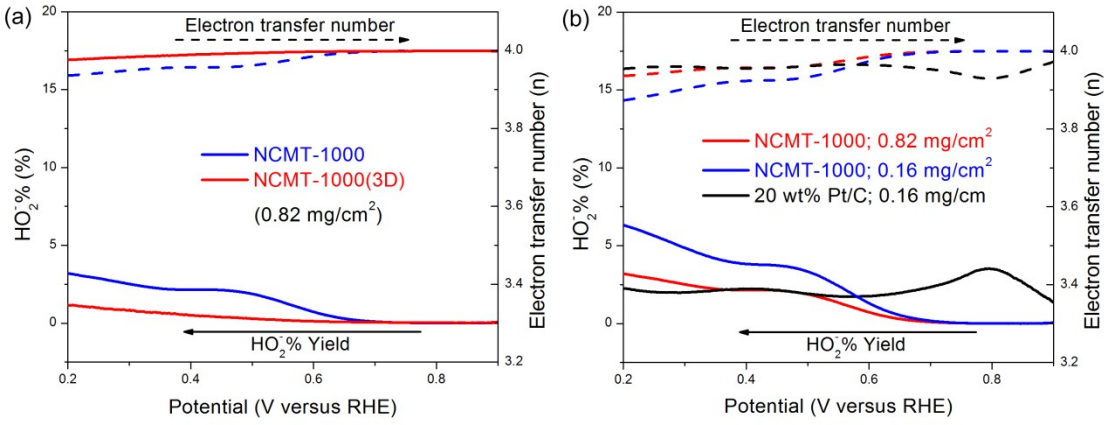

Fig. S7. Peroxide yield and electron transfer number obtained from the RRDE curves for the NCMT-1000 and commercial Pt/C catalysts.

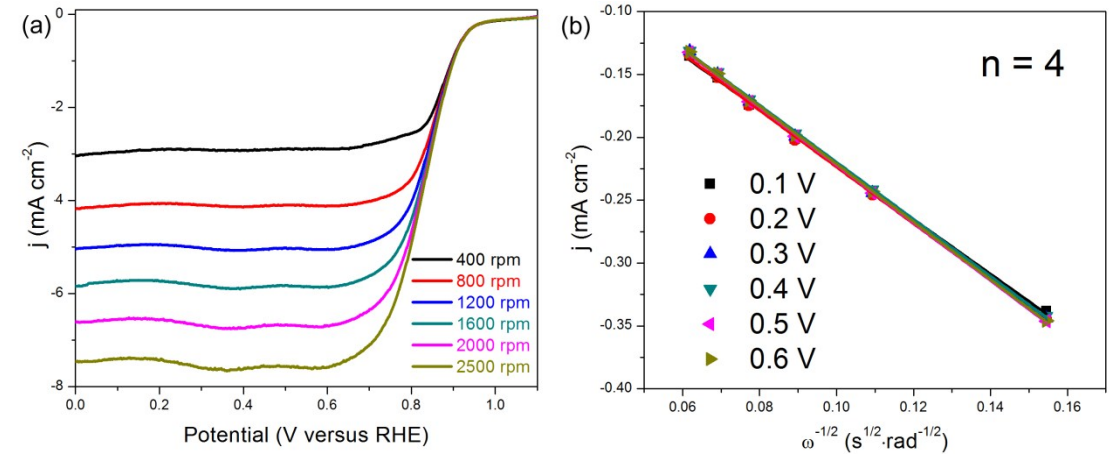

Fig. S8. RDE curves of NCMT-1000 at an RDE (1600 rpm) in an O_2-saturated 0.1 M KOH solution.

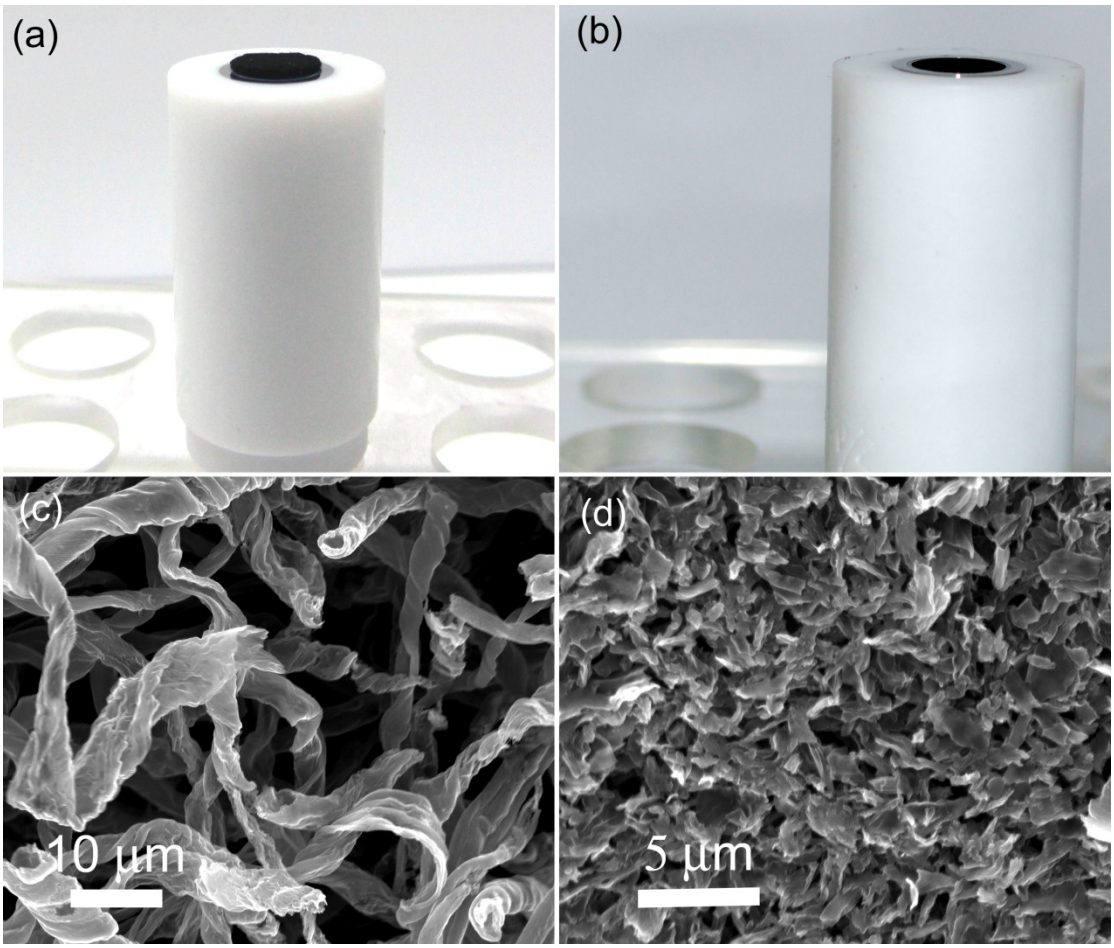

Fig. S9. (a, b) Optical and (c, d) cross-section SEM images of the (a, c) NCMT-1000(3D) and (b, d) NCMT-1000 electrodes.

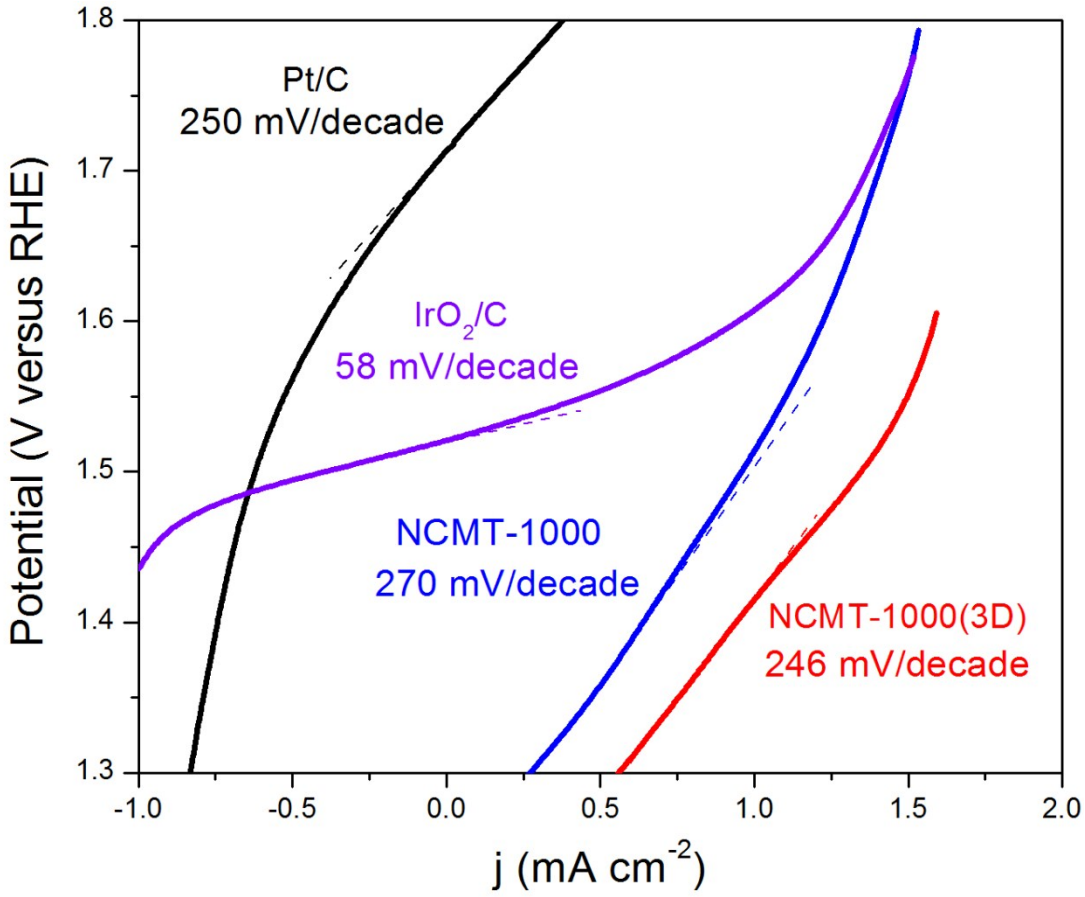

Fig. S10. Tafel plots of the NCMT-1000 materials, Pt/C and Ir/C.

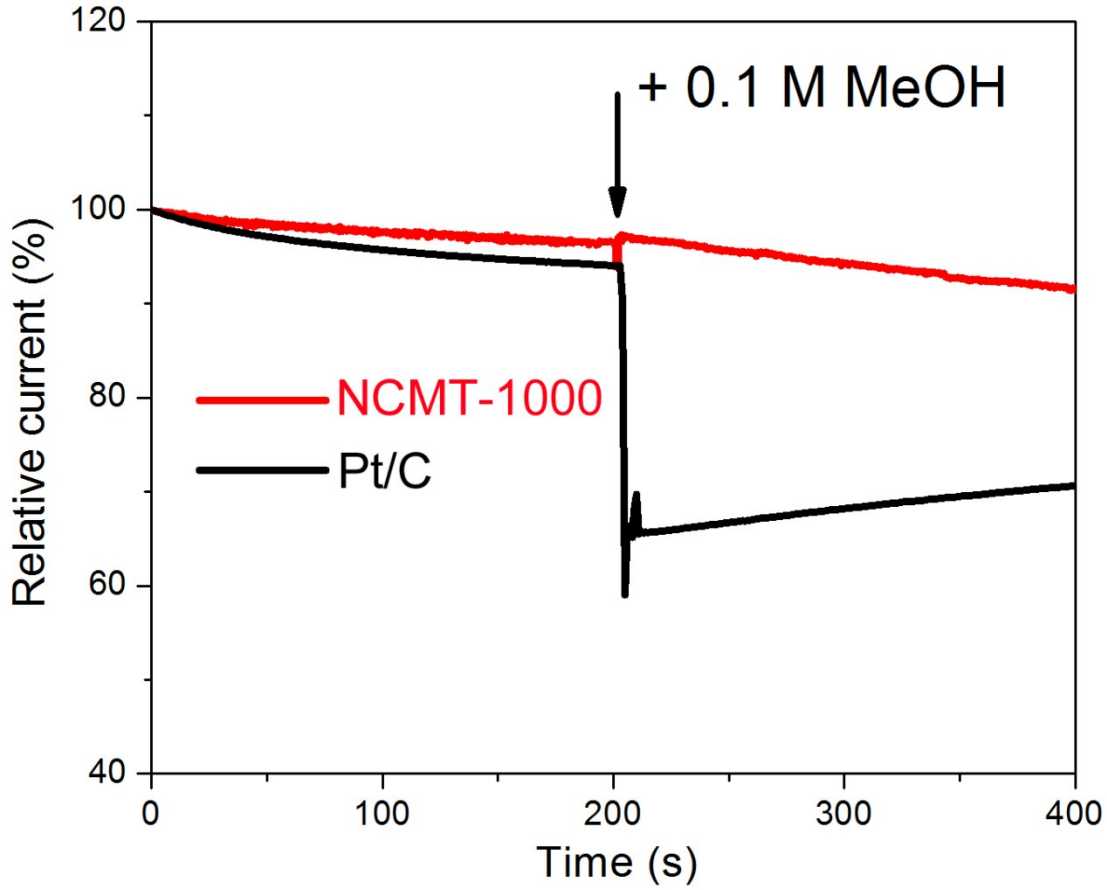

Fig. S11. The methanol-tolerance evaluation of NCMT-1000 and Pt/C tested by the chronamperometric responses.

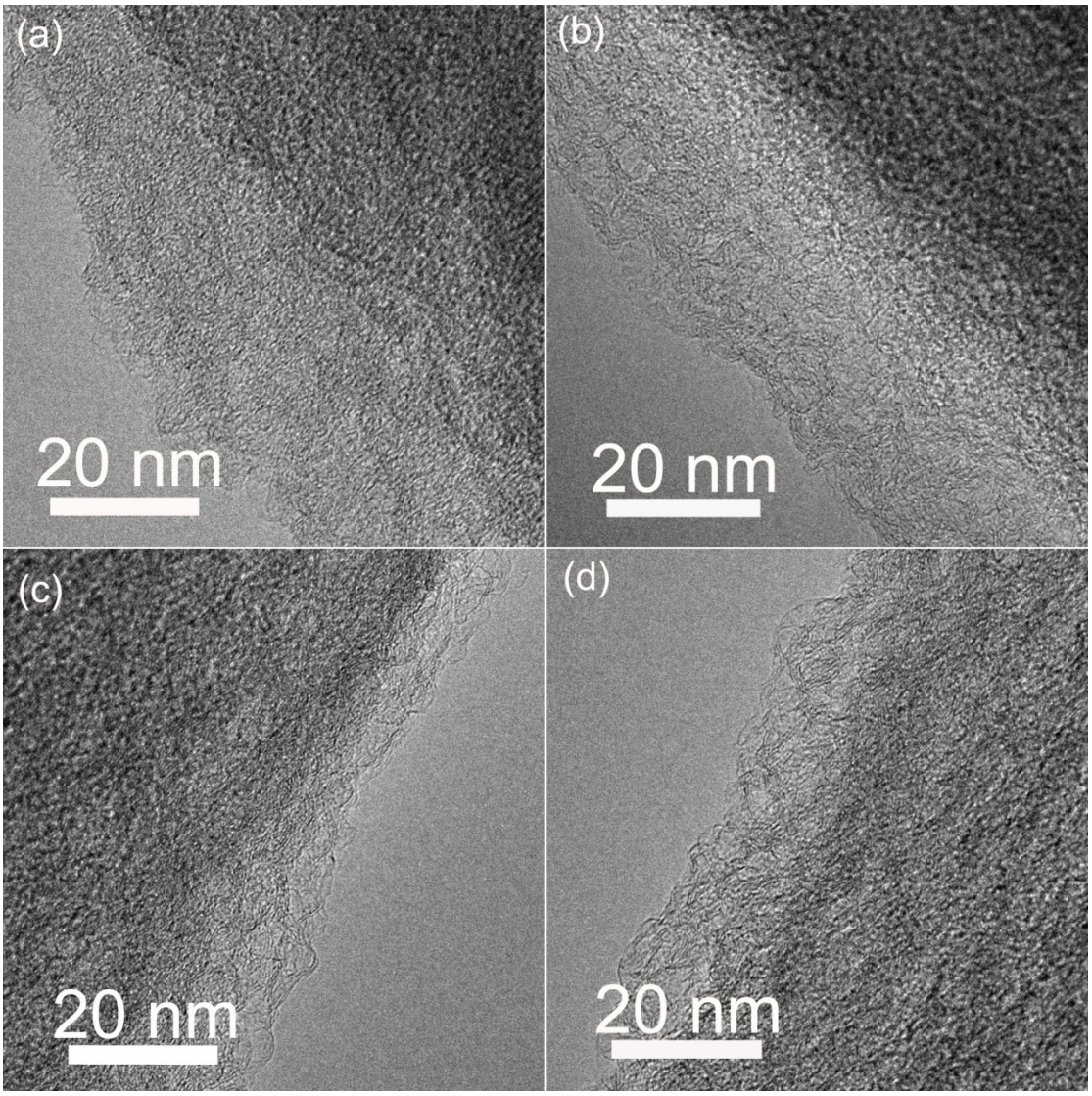

Fig. S12. TEM images of (a) NCMT-800, (b) NCMT-900, (c) NCMT-1000, and (d) NCMT-1100.

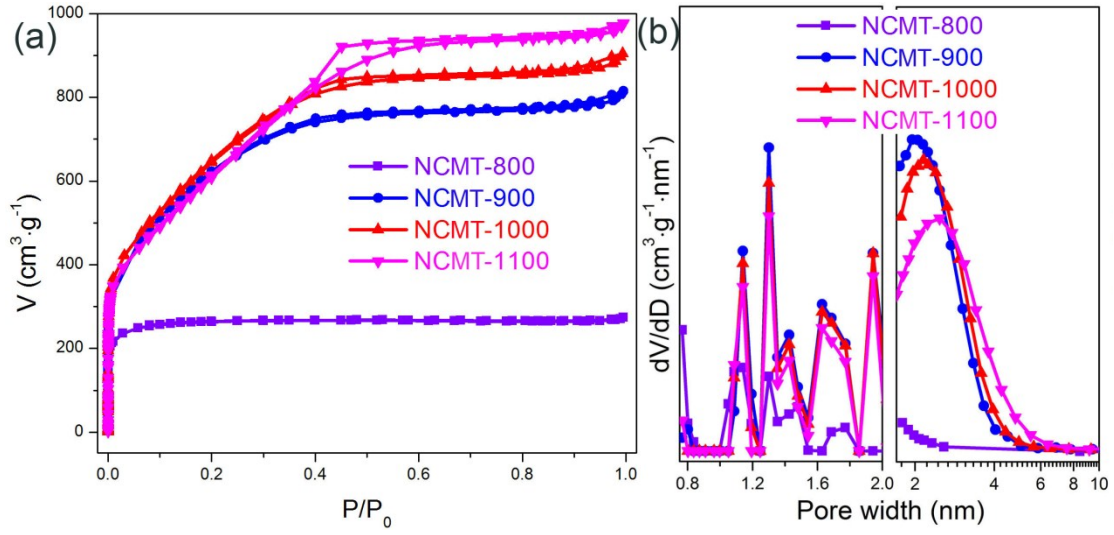

Fig. S13. (a) N_2 adsorption/desorption isotherms and (b) corresponding pore distributions of the NCMT materials.

The Raman spectra of the NCMTs show that the G-band and D-band peaks become slimmer with increasing treatment temperature (Fig. S14a) due to the formation of better crystalline graphitic domains.[1-3] TGA measurements (Fig. S14b) indicate that the rapid oxidation temperatures of the NCMTs increase with an increase in pyrolysis temperature, verifying that a higher pyrolysis temperature produces better graphitized carbon, consistent with the TEM and Raman characterizations. X-ray diffraction (XRD) patterns (Fig. S14c) show that the (002) peaks of the NCMTs become more asymmetric and broader with increasing annealing temperature, suggesting more single-layer or few-layer graphene domains are created at higher annealing temperatures.[4]

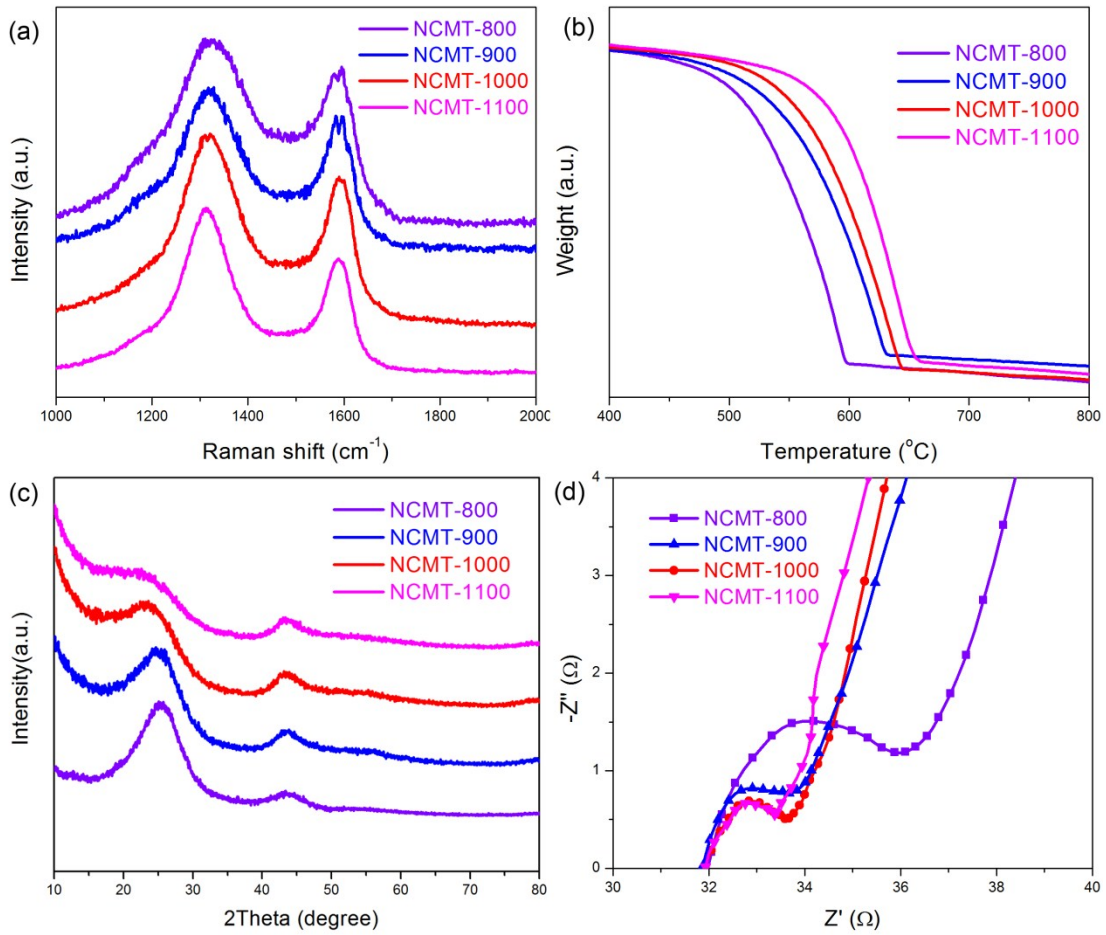

Fig. S14. (a) Raman spectra, (b) TGA curves, (c) XRD patterns, and electrochemical impedance spectra of the NCMT materials.

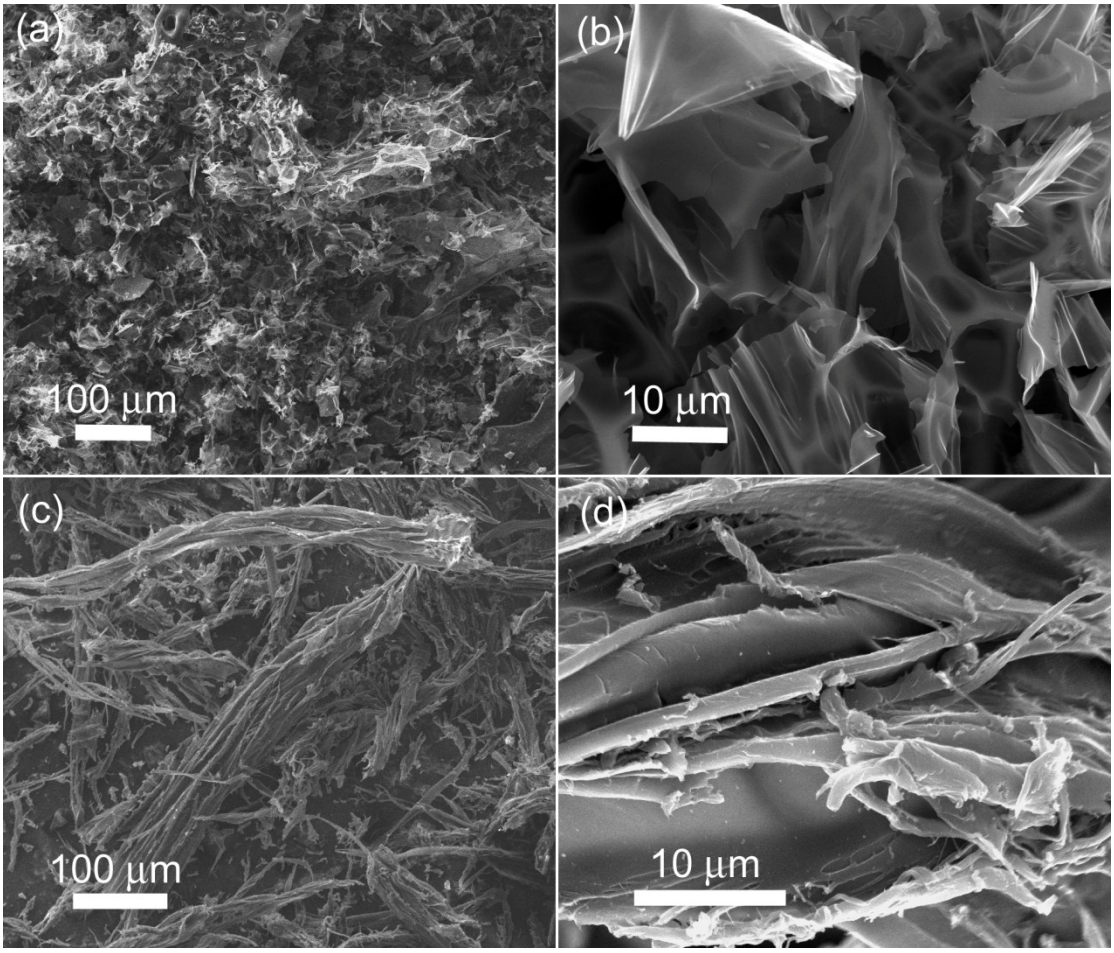

Fig. S15. SEM images of (a, b) NPGS-1000 and (c, d) NPCF-1000 prepared by using starch and saw dust as the respective raw materials.

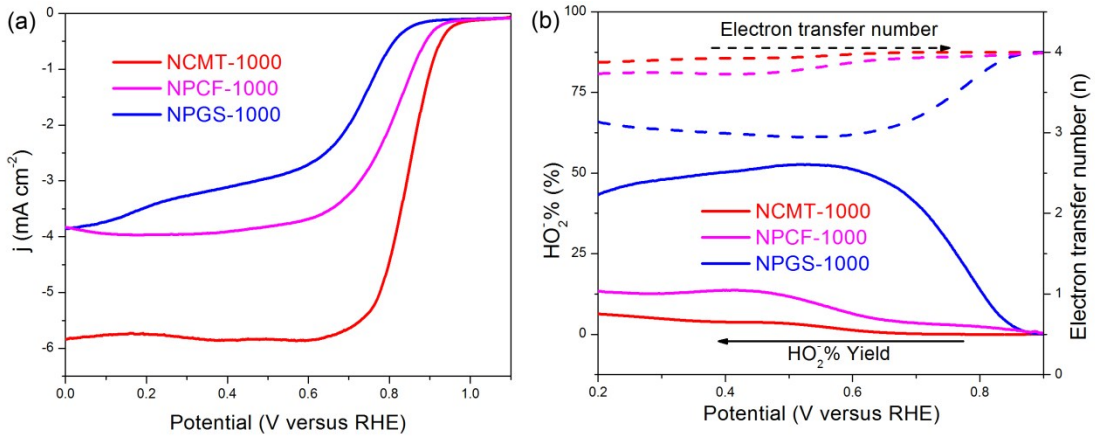

Fig. S16. (a) RRDE voltammograms recorded with NCMT-1000, NPGS-1000 and NPCF-1000 in an O_2-saturated 0.1 M KOH solution at 1600 rpm. (b) Peroxide yield and electron transfer number obtained from RRDE curves for NCMT-1000, NPGS-1000 and NPCF-1000.

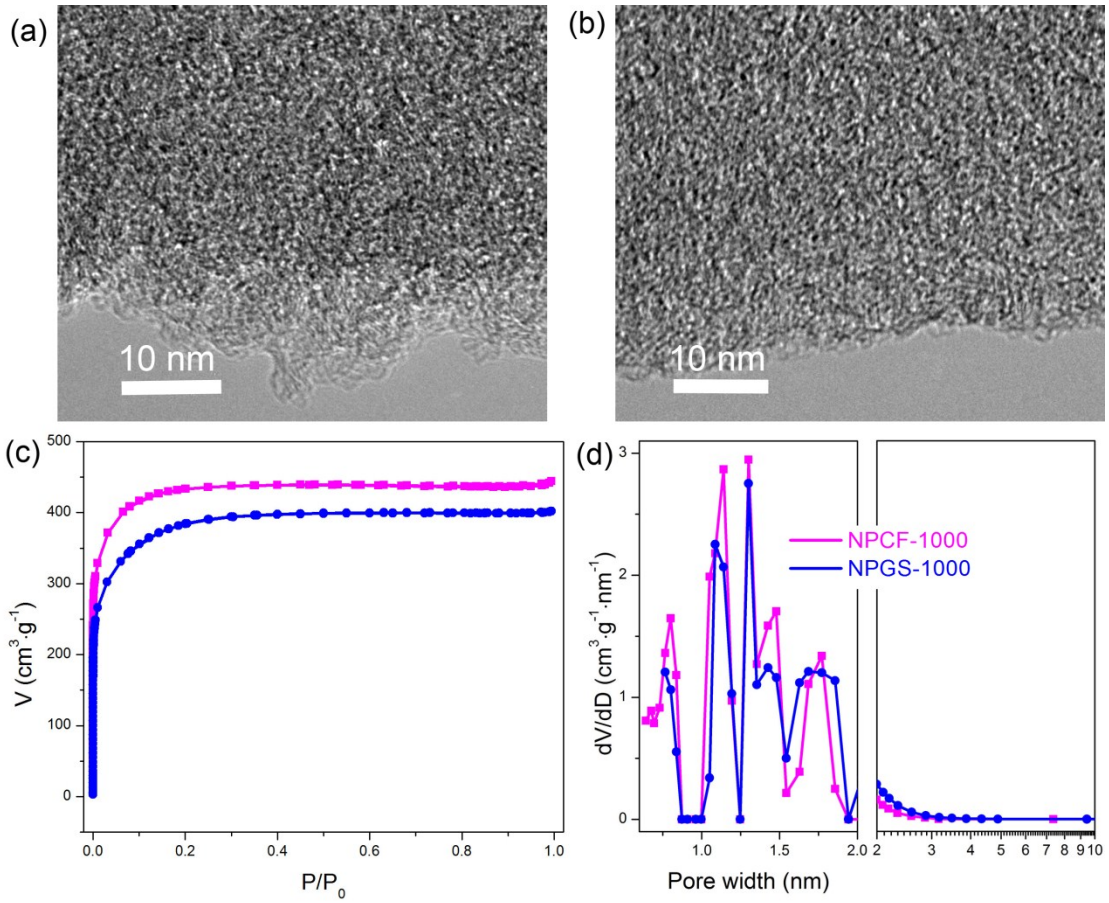

Fig. S17. TEM images of (a) NPGS-1000 and (b) NPCF-1000. (c) N_2 adsorption/desorption isotherms and (d) corresponding pore distributions of NPGS-1000 and NPCF-1000.

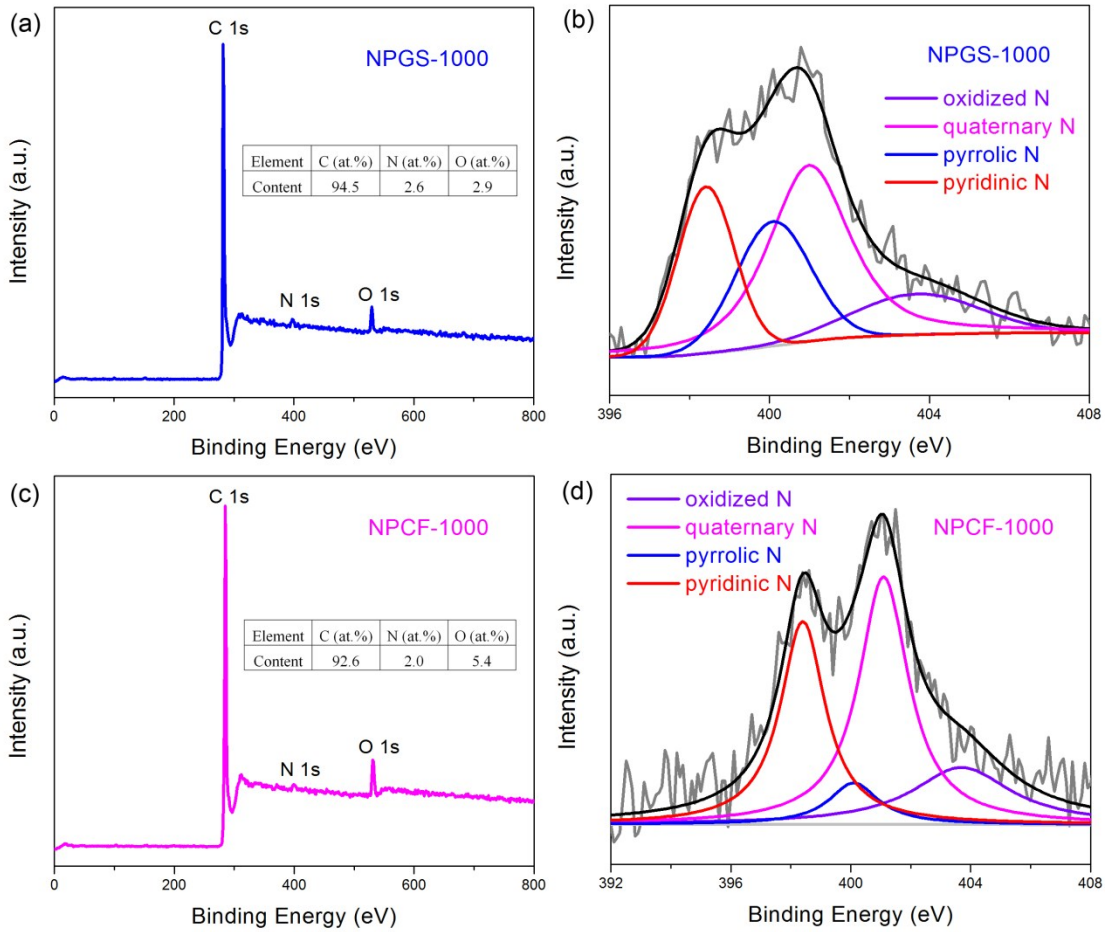

Fig. S18. XPS spectra of (a, b) NPGS-1000 and (c, d) NPCF-1000.

Table S1 A summary of the ORR catalytic activities of some previously reported metal-free carbon-based catalysts and our NCMT-1000 materials (as measured in 0.1 M KOH, electrode rotation speed: 1600 rpm)

Material	Catalyst loading (mg cm^{-2})	S_{BET} (m^2 g)	E_{onset} (V)	$E_{1/2}$ (V)	J at 0.8 V (mA cm^{-2})	Reference
VA-NCNTs	unknown	-	-	0.84	2.65	Science 2009, 323, 760
NCNC700/900	0.1	884	0.84	0.71	0.5	Adv. Mater. 2012, 24, 5593
NG	0.037	816	0.92	0.71	1.15	Adv. Funct. Mater. 2012, 22, 3634-3640
Meso/micro-P*o*PD	0.1	1280	-	0.85	4.32	Nat. Commun. 2014, 5
CNT/HDC-1000	0.6	325	0.92	0.82	3.40	Angew. Chem. Int. Ed. 2014, 53, 4102-4106
NPOMC-L1	0.3	1100	0.92	0.82	Ca. 3.0	Angew. Chem. Int. Ed. 2015, 54, 9230-9234
NPMC-1000	0.15	1548	0.94	0.85	Ca. 3.5	Nat. Nano. 2015, 10, 444-452
N-CNF aerogel	0.4	916	-	0.80	2.57	Nano Energy. 2015, 11, 366-376
TTF-F	0.3	2570	0.86	0.77	Ca. 2.0	Adv. Mater. 2015, 27, 3190-3195
NCMT-1000	**0.16**	**2358**	**1.02**	**0.845**	**4.45**	**This work**
NCMT-1000	**0.82**		**1.03**	**0.860**	**4.97**	
NCMT-1000(3D)	**0.82**		**1.05**	**0.710**	**8.70**	
Pt/C	**0.16**	**-**	**1.02**	**0.830**	**4.20**	

Table S2 Elemental composition, specific surface area, and pore volume of NCMTs, NPGS-1000, and NPCF-1000.

sample	S_{BET} (m^2 g^{-1})	Micropore volume (cm^3 g^{-1})	Mesopore volume (cm^3 g^{-1})	C (at%)	N (at%)	O (at%)	Pyridinic and quaternary N (at.%)
NCMT-800	801	0.38	0.03	88.7	6.0	5.3	3.9
NCMT-900	2203	0.67	0.54	90.2	4.1	5.7	2.8
NCMT-1000	2358	0.70	0.64	93.2	2.0	4.8	1.5
NCMT-1100	2300	0.69	0.78	95.4	1.3	3.3	1.0
NPGS-1000	1200	0.48	0.14	94.5	2.6	2.9	1.6
NPCF-1000	1315	0.58	0.09	92.6	2.0	5.4	1.5

Table S3 ORR performance of the NCMT and Pt/C catalysts (catalyst loading was 0.16 mg cm^{-2})

sample	E_{onset} (V, RHE)	$E_{1/2}$ (V, RHE)	J at 0.8 V (mA cm^{-2})	n*
NCMT-800	0.97	0.715	0.95	3.66
NCMT-900	1.00	0.800	2.39	3.84
NCMT-1000	1.02	0.845	4.45	3.95
NCMT-1100	1.00	0.810	2.58	3.78
Pt/C	1.02	0.829	4.20	3.95

Note: *(Electron transfer number (n) was an averaged value calculated over the potential range 0.2-0.9 V from RRDE measurements).

1. J.-C. Li, S.-Y. Zhao, P.-X. Hou, R.-P. Fang, C. Liu, J. Liang, J. Luan, X.-Y. Shan and H.-M. Cheng, *Nanoscale*, 2015, **7**, 19201-19206.
2. J. Zhang, Z. Zhao, Z. Xia and L. Dai, *Nat. Nanotechnol.*, 2015, **10**, 444-452.

3. R. Sharma and K. K. Kar, *J. Mater. Chem. A*, 2015, **3**, 11948-11959.
4. D. N. Futaba, T. Yamada, K. Kobashi, M. Yumura and K. Hata, *J. Am. Chem. Soc.*, 2011, **133**, 5716-5719.